Low-energy theorems for nucleon-nucleon scattering at $M_\pi = 450$ MeV

V. Baru,[1,2] E. Epelbaum,[1] and A. A. Filin[1]
[1]*Institut für Theoretische Physik II, Ruhr-Universität Bochum, D-44780 Bochum, Germany*
[2]*Institute for Theoretical and Experimental Physics, B. Cheremushkinskaya 25, 117218 Moscow, Russia*
(Received 15 April 2016; published 11 July 2016)

We apply the low-energy theorems to analyze the recent lattice QCD results for the two-nucleon system at a pion mass of $M_\pi \simeq 450$ MeV obtained by the NPLQCD Collaboration. We find that the binding energies of the deuteron and dineutron are inconsistent with the low-energy behavior of the corresponding phase shifts within the quoted uncertainties and vice versa. Using the binding energies of the deuteron and dineutron as input, we employ the low-energy theorems to predict the phase shifts and extract the scattering length and the effective range in the $^3S_1$ and $^1S_0$ channels. Our results for these quantities are consistent with those obtained by the NPLQCD Collaboration from effective field theory analyses but are in conflict with their determination based on the effective-range approximation.

DOI: 10.1103/PhysRevC.94.014001

I. INTRODUCTION

Understanding of certain fine-tunings in the parameters of the Standard Model is an important frontier in modern hadron and nuclear physics. In connection with anthropic considerations, a question has been raised whether the light quark masses have to take very specific values in order to maintain conditions essential for the development of life; see Ref. [1] for a discussion. In particular, the proximity of the Hoyle state, the first 0^+ excited state of ^{12}C, to the triple alpha-particle threshold is known to be crucial for the enhanced resonance formation of the life-important elements ^{12}C and ^{16}O in red giant stars [2]. The dependence of the excitation energy of the Hoyle state on the light-quark masses was analyzed recently within *ab initio* nuclear lattice simulations [3,4]. It was found that the variation of the light quark masses by a few percent is likely to be not detrimental for the development of life. More conclusive statements would require a better knowledge of the quark mass dependence of the nuclear force or, more precisely, of the nucleon-nucleon (NN) S-wave scattering lengths, which are by far the dominant source of theoretical uncertainty in this calculation. The quark mass dependence of the nuclear force also plays an important role in constraining a time variation of the Standard Model parameters as predicted by various extensions of the Standard Model at the time of Big Bang nucleosynthesis by comparing the observed and calculated primordial deuterium and helium abundances [5,6].

In recent years, there has been significant progress in lattice-QCD calculations of nuclear systems which constitute the primary source of information about the light-quark or, equivalently, pion mass dependence of nuclear observables. In particular, fully dynamical calculations at unphysical pion masses as low as $M_\pi \simeq 300$–400 MeV have been performed; see, e.g., Refs. [7–9]. To connect these results with experimentally observed quantities corresponding to the physical value of the quark masses one can employ chiral effective field theory (EFT), which is still expected to be applicable at such pion masses [6,10–17]. Notice that not only the binding energies but also the NN scattering observables such as the phase shifts and effective range parameters have been calculated on a lattice; see Refs. [9,18,19] for recent analyses of the NN $^1S_0$ and $^3S_1$ channels by the NPLQCD Collaboration at $M_\pi \simeq 450$ and 800 MeV and Ref. [20] for the analysis of the higher partial waves at $M_\pi \simeq 800$ MeV by the CalLat Collaboration. Interestingly, the general trend of lattice calculations by different groups suggests a stronger attraction both in the $^1S_0$ and $^3S_1$ channels when going away from the physical point towards heavier quark masses [7–9,19,21]. Both the deuteron and dineutron systems in these calculations are found to be bound at unphysically heavy pion masses, with the deuteron binding energy being significantly larger than the experimentally observed one. These results are, however, not supported by the HAL QCD Collaboration, which finds no bound states in these channels for pion masses ranging from 469 to 1171 MeV [22]. It should be noted that unlike the lattice calculations mentioned above, a different approach is employed by the HAL QCD Collaboration, which makes use of a two-nucleon potential at the intermediate step. The puzzle is even more intriguing given that the chiral EFT calculations tend to indicate less attraction at M_π larger than the physical value [6,10,12,13,17]; see also Ref. [23] for a related work. These calculations, however, rely on the naturalness assumption and/or make use of resonance saturation estimates for M_π-dependent four-nucleon contact interactions.

In our recent paper [24], we argued that the low-energy theorems (LETs) in NN scattering can provide important consistency checks of both lattice-QCD results and their chiral extrapolations. Specifically, knowledge of the analytic properties of the scattering amplitude allows one to predict its energy dependence and, under certain circumstances, extract the parameters of the effective range expansion. In Ref. [24], we tested this approach by predicting the effective range parameters for S-wave NN scattering in the spin-triplet and the spin-singlet channels; see also Refs. [25–30] for earlier studies along this line. Further, we generalized the LETs to unphysical pion masses and applied the resulting approach to selected lattice-QCD results. In particular, using the linear behavior of the quantity $M_\pi r$, where r refers to the effective range, conjectured in Ref. [19] and visualized in Fig. 1, we employed

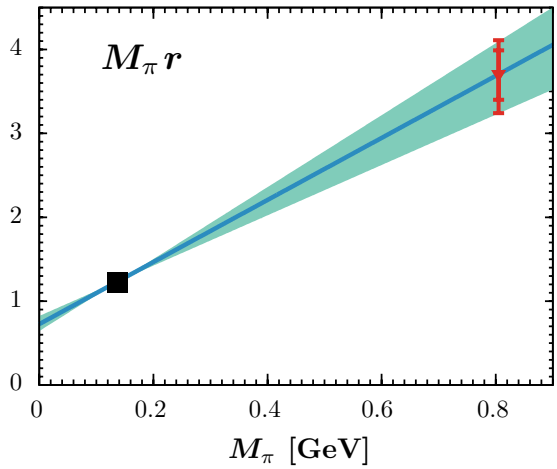

FIG. 1. Linear with M_π behavior of the effective range in units of pion mass $M_\pi r$ in the $^3S_1$ partial wave conjectured in Ref. [19]. Red solid triangle corresponds to the NPLQCD result at $M_\pi \simeq 800$ MeV [18] while the shaded area shows the uncertainty of the suggested linear interpolation. The black square shows the empirical value of the effective range at the physical pion mass [31].

the LETs to predict the M_π dependence of the deuteron binding energy and of the other parameters in the effective range expansion of the NN scattering amplitude in the $^3S_1$ channel. Remarkably, the resulting M_π dependence of the deuteron binding energy turned out to be in good agreement with the general trend of different lattice calculations [7–9,19,21], except for the results of Ref. [22] which do not support the existence of bound states for large pion masses.

Recently, the NPLQCD Collaboration reported their new results for the S-wave NN observables both in the spin-triplet and the spin-singlet channels at $M_\pi = 450$ MeV [9]. In particular, they have calculated the values of the deuteron and the dineutron binding energies and the phase shifts in the $^3S_1$ and $^1S_0$ channels at several values of the center-of-mass system (cms) momenta above threshold. In this paper we confront these results with the LETs. In particular, we demonstrate that the lattice phase shifts at the two lowest energies in the $^3S_1$ channel are inconsistent (within the quoted uncertainties) with the deuteron binding energy obtained in the same lattice calculation. The situation is less conclusive in the $^1S_0$ channel due to larger uncertainties of the LETs in this channel. However, the results of our analysis in this channel also indicate an inconsistency between the phase shifts and the large value of the dineutron binding energy reported by the NPLQCD Collaboration. Taking the NPLQCD results for the deuteron and dineutron binding energies as input, we use the LETs to infer the corresponding phase shifts and extract the values of the scattering lengths and effective ranges. We perform a detailed comparison of our results for these quantities with the ones of Ref. [9] and argue that their determination by means of the effective range approximation is not self-consistent.

Our paper is organized as follows. In Sec. II, we discuss in detail our formalism, explain the meaning of the LETs, and discuss their generalization to unphysical values of the pion mass. Implications of the LETs for the recent lattice-QCD results at $M_\pi \sim 450$ MeV are considered in Sec. III. Section IV addresses the dependence of the effective range on the pion mass. Finally, our main findings are summarized in Sec. V.

II. LOW-ENERGY THEOREMS FOR NN SCATTERING

A. The formalism at the physical pion mass

The concept of the low-energy theorems for NN scattering and their generalization to unphysical pion masses have been discussed in Ref. [24], see also Refs. [25–30] for related earlier studies. In this section we formulate the main idea of the LETs from a somewhat different perspective as compared to Ref. [24], where a quantum mechanical framework of the modified effective range expansion [32] was employed.

We assume that the NN interaction is characterized by two distinct scales M_L and M_S, $M_L \ll M_S$, so that the potential can be written as

$$V = V_L + V_S, \tag{2.1}$$

with the interaction ranges of the order of $r_L \sim M_L^{-1}$ and $r_S \sim M_S^{-1}$, respectively. The analytic structure of the scattering amplitude near threshold is governed by the long-range interactions. Taking into account the discontinuity across the left-hand cut from the long-range potential V_L, the energy dependence of the scattering amplitude can be predicted in a model-independent way up to the energies corresponding to the branch point of a more distant left-hand cut associated with the potential V_S. This prediction can be regarded as a low-energy theorem. Alternatively, one can view the LETs as correlations between the parameters in the effective-range expansion of the inverse scattering amplitude induced by long-range interactions. Notice that the inverse scattering amplitude may possess poles in the near-threshold region, whose appearance does not affect the validity range of the LETs if the scattering amplitude is kept unexpanded.

The longest-range part of the NN force is due to the one-pion exchange potential (OPEP). Thus, the LETs for NN scattering are expected to be governed by the left-hand cut generated by the OPEP. The OPEP is, however, singular at the origin and requires regularization and renormalization. Therefore, instead of using the quantum mechanical approach, we formulate the LET within the modified Weinberg approach of chiral EFT [17,24,33,34]. Since the correlations between the effective range expansion parameters are inherently long-range phenomena, the results after renormalization and removing the ultraviolet cutoff should be model and regularization-scheme independent.

To be specific, we calculate the scattering amplitude T by solving the Lippmann-Schwinger-type integral equation introduced originally by Kadyshevsky [35] which, for the case of the fully off-shell kinematics, has the form

$$T(\vec{p},\vec{p}\,',k) = V(\vec{p},\vec{p}\,') + \int d^3q\, V(\vec{p},\vec{q}\,)\, G(k,q)\, T(\vec{q},\vec{p}\,',k), \tag{2.2}$$

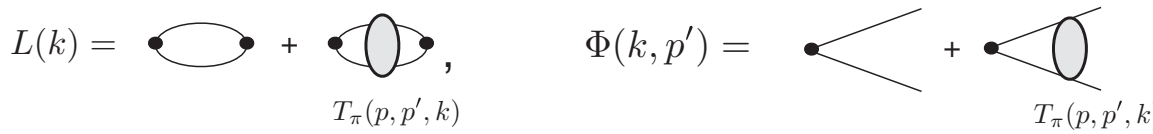

FIG. 2. Graphical illustration of the functions Φ and L in Eq. (2.6), which correspond to convolutions of the pionic amplitude T_π with the pointlike vertices as explained in the text.

where $G(k,q)$ is the free Green function,

$$G(k,q) = \frac{m_N^2}{2(2\pi)^3} \frac{1}{\left(\vec{q}^{\,2} + m_N^2\right)\left(E_k - \sqrt{\vec{q}^{\,2} + m_N^2} + i\epsilon\right)}. \tag{2.3}$$

Further, $\vec{p}$ ($\vec{p}\,'$) is the incoming (outgoing) three-momentum of the nucleon in the cms and $E_k = \sqrt{\vec{k}^{\,2} + m_N^2}$ with m_N denoting the nucleon mass and $\vec{k}$ being the corresponding (on-mass-shell) three-momentum. The S-wave potential at leading order (LO) consists of the OPEP and two derivativeless contact interactions (here denoted C_0 for each given partial wave)

$$V_{\rm LO}(\vec{p},\vec{p}\,') = -\frac{g_A^2}{4F_\pi^2} \frac{\vec{\sigma}_1 \cdot (\vec{p} - \vec{p}\,')\vec{\sigma}_2 \cdot (\vec{p} - \vec{p}\,')}{(\vec{p} - \vec{p}\,')^2 + M_\pi^2} \boldsymbol{\tau}_1 \cdot \boldsymbol{\tau}_2 + C_0, \tag{2.4}$$

where $\vec{\sigma}_i$ ($\boldsymbol{\tau}_i$) denote the spin (isospin) Pauli matrices of the nucleon i, while g_A and F_π refer to the axial vector coupling of the nucleon and the pion decay constant, respectively. As discussed in Ref. [33], the LO integral equation in this framework is exactly renormalizable,[1] that is, all ultraviolet divergencies appearing from iterations of the LO potential can be removed via an appropriate redefinition of the contact interaction C_0. As a consequence, the cutoff in the integral equation can be put to infinity, so that no finite-cutoff artifacts can affect the LET.

The numerical solution of the integral equation (2.2) is carried out to obtain the full quantitative results for the correlations implied by the LETs for the single- ($^1S_0$) and coupled-channel ($^3S_1$–$^3D_1$) problems. While the integral equation (2.2) with the potential (2.4) can, in general, be only solved numerically, the correlations between the parameters of the effective range expansion implied by the LETs can be demonstrated analytically. To make this demonstration more transparent, we consider the partial wave projected T matrix in an uncoupled channel with the zero orbital angular momentum, whereas generalizations to the coupled-channel case and to nonzero angular momenta are straightforward.

Since the LO contact interaction is separable, it is possible to write the solution for the T matrix in the semianalytic (operator) form

$$\begin{aligned} T(p,p',k) &= T_\pi(p,p',k) + \Phi(p,k)\, D(k)\, \Phi(k,p'), \\ D(k) &= \frac{1}{C_0^{-1} - L(k)}, \end{aligned} \tag{2.5}$$

where $T_\pi(p,p',k)$ denotes the off-shell solution of the projected integral equation (2.3) with the OPEP alone ($C_0 = 0$), whereas the functions Φ and L, shown graphically in Fig. 2, involve convolutions of this pionic amplitude with the pointlike vertex, namely

$$\begin{aligned} \Phi(k,p') &= 1 + \int dq\, q^2\, G(k,q)\, T_\pi(q,p',k), \\ \Phi(p,k) &= 1 + \int dq\, q^2\, T_\pi(p,q,k)\, G(k,q), \\ L(k) &= \int dq\, q^2\, G(k,q) + \int dq\, dq'\, q^2\, q'^2\, G(k,q) \\ &\quad \times T_\pi(q,q',k)\, G(k,q'). \end{aligned} \tag{2.6}$$

To complete the renormalization program at LO, one has to express the contact interaction C_0 in terms of the scattering amplitude at zero momentum; that is, the scattering length a, which is assumed to be an input quantity. Thus, the on-shell NN amplitude reads

$$\begin{aligned} T(k) &= T_\pi(k) + \Phi(k)\, D(k)\, \Phi(k), \\ D(k) &= \frac{1}{\frac{\Phi^2(0)}{T(0) - T_\pi(0)} + L(0) - L(k)}, \\ T(0) &= -\frac{16\pi^2}{m_N} a, \end{aligned} \tag{2.7}$$

where we used the shorthand notation $T(k) \equiv T(k,k,k)$, $\Phi(k) \equiv \Phi(k,k)$.

For an uncoupled channel with the zero orbital angular momentum, the scattering amplitude $T(k)$ can be expressed in terms of the so-called effective range function $F(k) \equiv k \cot \delta(k)$ via

$$T(k) = -\frac{16\pi^2}{m_N} \frac{1}{F(k) - ik}. \tag{2.8}$$

We are now in the position to formulate the LETs at LO: Using the scattering length as the only input quantity to fix the unknown low-energy constant, we employ Eqs. (2.7)–(2.8) to predict the momentum dependence of the scattering amplitude and to calculate the phase shifts $\delta(k)$. Such a prediction is possible because all information about the longest-range OPE potential and, in particular, about the discontinuity across the

[1]For a recent extension of the approach to $\bar{D}D^*$ scattering see Ref. [36]. This paper also addresses chiral extrapolations of the $X(3872)$ binding energy.

corresponding left-hand cut starting from the momentum $k = \pm i M_\pi/2$, is explicitly taken into account in the calculation.

Unlike the scattering amplitude, the effective range function does not possess the kinematic unitarity cut and is a real meromorphic function of k^2 near the origin $k = 0$ [37,38]. It can, therefore, be Taylor expanded about the origin, leading to the effective range expansion[2]

$$k \cot \delta(k) = -\frac{1}{a} + \frac{1}{2} r k^2 + v_2 k^4 + v_3 k^6 + v_4 k^8 + \cdots , \tag{2.9}$$

where r is the effective range, while v_i are the so-called shape parameters. Thus, a single piece of information in the form of the scattering length (or the energy of a bound/virtual state) allows one to predict all the coefficients in the effective range expansion:

$$r = \frac{\alpha(a M_\pi)}{M_\pi}, \quad v_i = \frac{\beta_i(a M_\pi)}{M_\pi^{2i-1}}, \tag{2.10}$$

where α and β_i are polynomials in the inverse scattering length, namely

$$\alpha = \alpha_0 + \frac{\alpha_1}{(a M_\pi)} + \frac{\alpha_2}{(a M_\pi)^2}, \tag{2.11}$$

$$\beta_i = \beta_{i,0} + \frac{\beta_{i,1}}{(a M_\pi)} + \frac{\beta_{i,2}}{(a M_\pi)^2} + \cdots + \frac{\beta_{i,i+1}}{(a M_\pi)^{i+1}}, \tag{2.12}$$

with the coefficients α_i and $\beta_{i,j}$ being calculable from the various quantities appearing in Eq. (2.7) and their derivatives evaluated at $k = 0$. Their explicit form can be easily obtained by performing Taylor expansion of the inverse amplitude T^{-1} around $k^2 = 0$.

Given that the left-hand cut from the OPEP is explicitly included, the convergence radius of the LETs is restricted by the next-to-lowest-lying left-hand singularity associated with the two-pion exchange potential (TPEP). In the present analysis, we take into account the contributions of the TPEP implicitly by including the relevant momentum-dependent short-range interactions at next-to-leading order (NLO), whose strengths have to be adjusted to reproduce the empirical value of the effective range in the corresponding channel. Then, the shape parameters can be predicted up to and including the NLO corrections.

After renormalization, the predictions for the LETs become insensitive to details of the short-range interaction once its strength is adjusted to reproduce the physical observable. As argued in Ref. [24], it is convenient to employ resonance saturation via a heavy-meson exchange in order to model higher-order contact interaction without destroying explicit renormalizability of the integral equation or having to rely on perturbation theory. Specifically, the NLO correction to the potential is taken in the form

$$V_{\rm NLO}(\vec{p}, \vec{p}\,') = \beta \, \frac{\vec{\sigma}_1 \cdot (\vec{p} - \vec{p}\,') \, \vec{\sigma}_2 \cdot (\vec{p} - \vec{p}\,')}{(\vec{p} - \vec{p}\,')^2 + M^2}, \tag{2.13}$$

where the heavy-meson mass M is set to be $M = 700$ MeV and the strength β is adjusted to reproduce the empirical value of the effective range in the ${}^1S_0$ and the ${}^3S_1$ channels. Our results are not sensitive to the functional form of the term parametrizing the subleading short-range interaction in Eq. (2.13); see Ref. [24] for more details.

We now summarize the main findings of Ref. [24] for the physical value of the pion mass:

(1) In the ${}^3S_1$ channel, the LETs yield very accurate results already at LO. For example, the effective range is predicted with an accuracy better than 10%. The accuracy at LO even appears to be better than one could naively expect from the ratio of scales corresponding to the explicitly included lowest left-hand cut from the OPEP and the next-to-lowest one from the TPEP, which is not considered explicitly at this order. This observation can be understood by noticing that iterations of the OPEP do actually generate the dominant contributions to the left-hand cuts due to the two- and multiple-pion exchange.

(2) The accuracy of the LETs in the ${}^1S_0$ channel is much worse than in the spin-triplet case. This has to be expected due to the weakness of the OPEP in that channel. Indeed, the OPEP contributes less than 20% to the magnitude of the empirical ${}^1S_0$ phase shift at its maximum value.

(3) As expected, the predicted values of the shape parameters at NLO show in both channels a clear improvement as compared with the LO results. In particular, the NLO LETs appear to be accurate at the level of a few percent for the ${}^3S_1$ channel (except for v_2 which is unnaturally small), while the accuracy of the predictions in the ${}^1S_0$ channel is improved to $\sim$25%.

B. Generalization to unphysical pion masses

A generalization of the LETs to the case of unphysical pion masses can be carried out straightforwardly [24]. The main dynamical effect of changing the pion mass in the OPEP corresponds to shifts of the branch points of all left-hand cuts. The discontinuity across the left-hand cuts also changes due to the dependence of the ratio g_A/F_π, which determines the strength of the OPEP, on the pion mass[3] M_π. Finally, the discontinuity across the left-hand cuts is also affected by the M_π-dependence of the nucleon mass through its appearance in the integral equation (2.2). To account for the last two effects in a way that minimizes the theoretical uncertainty, we use lattice-QCD results for the M_π dependence of g_A, F_π, and m_N. In

[2] We assume here that the phase shift does not cross zero in the region of validity of the effective range expansion. If this is the case, the Taylor expansion should be replaced by, e.g., the Padé approximation or the amplitude should be kept unexpanded; see Ref. [39] for a related discussion.

[3] We do not take into account the Goldberger-Treiman discrepancy in our analysis. For not too heavy pion masses, we expect the uncertainty in the strength of the OPEP to be dominated by the current uncertainty in the lattice-QCD calculations of g_A.

particular, we performed quadratic polynomial regression fits (as functions of M_π^2) of the lattice-QCD data for pion masses up to $M_\pi = 500$ MeV as shown in Fig. 3 of Ref. [24]. We refer the reader to this paper for more details on the fits and references to the included lattice-QCD calculations of these quantities. Using the above results, we can generalize the LO LETs by calculating the effective range function $F(k)$, see Eq. (2.8), as a function of the (inverse) scattering length at *arbitrary* values of the pion mass. Using a single input quantity such as the binding energy or the scattering length, we can then predict the phase shifts and extract the effective range r and the shape parameters v_i (provided the effective range function does not have poles near the origin). Some exemplary results for such predictions are discussed in Ref. [24] for different values of the pion mass. Notice that contrary to the chiral extrapolations performed in the framework of chiral EFT, no assumptions about the short-range interaction C_0 as a function of the pion mass is made when calculating the LETs. Instead, we perform fully independent calculations at each given value of the pion mass as if we lived in different worlds characterized by a specific value of M_π. Thus, for each considered value of the pion mass, the low-energy constant C_0 has to be adjusted to reproduce the given value of the scattering length used as input. By providing relations between various low-energy observables at unphysical values of the pion mass, the LETs may serve as consistency checks of the lattice QCD calculations.

As already emphasized above, the extension of the LETs to NLO is achieved by including subleading contact interactions parametrized via resonance saturation; see Eq. (2.13). Retaining the light-quark mass variation in the subleading contact interaction is formally suppressed according to the chiral EFT estimates. On the other hand, allowing for a variation of this term with M_π can be used to estimate the theoretical uncertainty of our analysis. Following Ref. [24], this is achieved by adjusting the strength β of the short-range interaction to reproduce the effective range at the physical point and by assuming that the M_π^2 dependence of β is within the envelope built by the straight lines which go through the physical point and describe a $\pm 50\%$ change in the value of β for $M_\pi = 500$ MeV, i.e.,

$$1 - \delta\beta \left| \frac{M_\pi^2 - \left(M_\pi^{\rm phys}\right)^2}{\Delta M_\pi^2} \right| \leqslant \frac{\beta(M_\pi)}{\beta\left(M_\pi^{\rm phys}\right)} \leqslant 1 + \delta\beta \left| \frac{M_\pi^2 - \left(M_\pi^{\rm phys}\right)^2}{\Delta M_\pi^2} \right|, \tag{2.14}$$

with $\delta\beta = 0.5$ and $\Delta M_\pi^2 \equiv (M_\pi^2 - (M_\pi^{\rm phys})^2)|_{M_\pi = 500\,\rm MeV}$. Such a choice of $\delta\beta$ is motivated by the fact that it would cover the known M_π dependence of g_A, F_π, and m_N if the same procedure is applied to these quantities. In the next section, we will also give results corresponding to the more conservative choice of $\delta\beta = 1.0$.

III. APPLICATION OF THE LETS TO THE NPLQCD RESULTS AT $M_\pi \sim 450$ MEV

As explained in the previous section, the LETs allow one to perform consistency checks of lattice-QCD results for NN scattering provided more than a single observable is extracted. Unfortunately, most of the lattice calculations in the NN sector have so far focused on the determination of the binding energies. One exception is the work by the NPLQCD Collaboration at the pion mass of $M_\pi \sim 800$ MeV [19], which provides, in addition to the binding energies, also the values of the scattering length, effective range and even the first shape parameter. It is, furthermore, conjectured in that paper that the effective range, expressed in units of the pion mass, may be approximated by a linear function of M_π. While the LETs are certainly beyond their range of applicability at such heavy pion masses, this conjecture was tested using the LETs in our previous work [24], where the resulting M_π dependence of the deuteron binding energy was indeed found to be in good agreement with the general trend of lattice data [7–9,19,21].

Recently, new results for NN scattering in the $^3S_1$ and $^1S_0$ channels were reported by the NPLQCD Collaboration at $M_\pi \sim 450$ MeV [9]. The calculations were performed for $n_f = 2 + 1$ flavors of light quarks at three lattice volumes of $L = 2.8$ fm, $L = 3.7$ fm, and $L = 5.6$ fm using the lattice spacing of $b = 0.12$ fm. In analogy to their previous work, the scattering phase shifts for the $^3S_1$ and $^1S_0$ partial waves were extracted for several values of the cms NN momenta using the extended Lüscher approach [40–42], as shown by the black filled regions in Fig. 3 for the case of the $^3S_1$ channel.

In addition to the phase shifts, the binding energies of the deuteron and the dineutron were extracted. Thus, it is interesting to test whether these results fulfill the LETs introduced above.

A. The $^3S_1$ channel

The deuteron binding energy calculated in Ref. [9] at $M_\pi \simeq 450$ MeV at three lattice volumes and extrapolated to the infinite volume is

$$B_d = 14.4\left(^{+3.2}_{-2.6}\right)\ \text{MeV}, \tag{3.1}$$

where the errors include statistical and systematic uncertainties as well as the extrapolation uncertainty combined in quadrature. Further, the first two coefficients in the effective range expansion, namely the scattering length and the effective range, were determined in Ref. [9] by fitting the effective range approximation of the effective range function,

$$k \cot\delta \simeq -\frac{1}{a} + \frac{1}{2} r k^2, \tag{3.2}$$

to the two lowest-energy scattering data points and the deuteron binding energy; see the grey bands in the right panel of Fig. 3. Notice that all three lattice data correspond to nucleon momenta below the branch point $|k| = M_\pi/2$ of the left-hand cut from the OPEP. The resulting values for the inverse scattering length and the effective range in units of the pion mass reported in Ref. [9] are

$$\begin{aligned} \left(M_\pi a^{(^3S_1)}\right)^{-1} &= -0.04\left(^{+0.07}_{-0.10}\right)\left(^{+0.08}_{-0.17}\right), \\ M_\pi r^{(^3S_1)} &= 7.8\left(^{+2.2}_{-1.5}\right)\left(^{+3.5}_{-1.7}\right), \end{aligned} \tag{3.3}$$

where the uncertainties in the first and second parentheses are statistical and systematic, respectively.

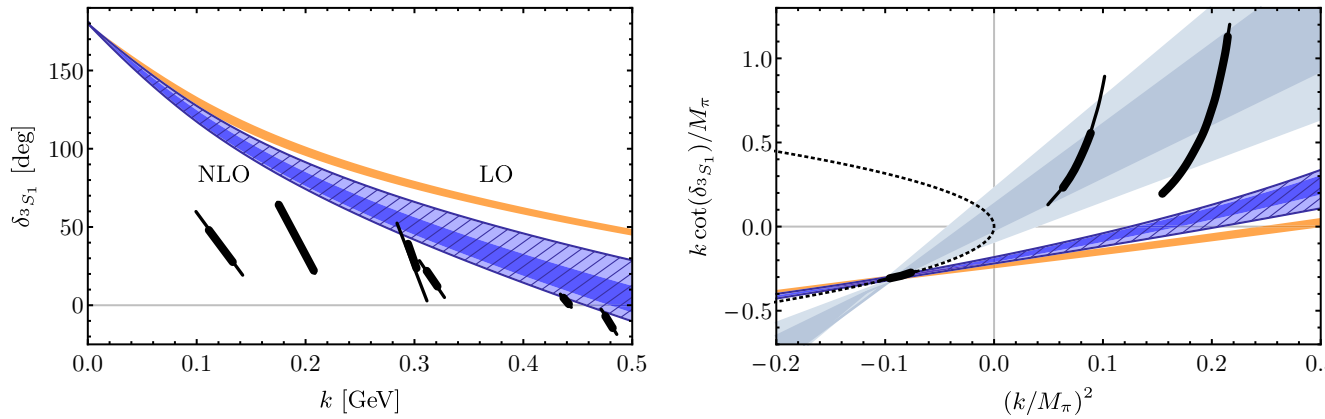

FIG. 3. Neutron-proton phase shifts (left panel) and the effective-range function (right panel) in the $^3S_1$ channel calculated on the lattice at $M_\pi \sim 450$ MeV [9] (filled black regions) in comparison with the predictions based on the LETs at LO (orange light-shaded bands) and NLO (blue dark-shaded and hatched blue light-shaded bands) using the NPLQCD result for the deuteron binding energy B_d as input. The uncertainty at LO shown by the orange bands is entirely given by the uncertainty of B_d in Eq. (3.1). The NLO dark-shaded (hatched light-shaded) bands correspond to the uncertainty in B_d and the theoretical uncertainty of the LETs estimated via the variation of β with $\delta\beta = 0.5$ ($\delta\beta = 1.0$) combined in quadrature. The grey light- and dark-shaded bands in the right panel depict the fit results of the lattice points of Ref. [9] based on the effective range approximation. The energy of the bound (virtual) states corresponds to the intersection points of the effective-range function $k\cot\delta^{(^3S_1)}$ and the unitarity term $ik/M_\pi = \pm\sqrt{-(k/M_\pi)^2}$, shown by the dotted line in the right panel, in the lower (upper) half-plane. The phase shift corresponds to the Blatt-Biedenharn parametrization of the S matrix [43].

In Fig. 3, we confront the lattice-QCD phase shifts of Ref. [9] with the predictions of the LETs at LO and NLO. We use the NPLQCD result for the deuteron binding energy given in Eq. (3.1) as input to adjust the leading-order contact term C_0. This is sufficient to predict the phase shift at LO. As explained in the previous section, there are no additional parameters at NLO. As shown in the left panel of Fig. 3, the change in the phase shifts when going from LO to NLO is reasonably small, which confirms a good convergence of the LETs in this channel. The expected accuracy of the NLO prediction can be roughly estimated by the width of the blue band generated by the variation of the parameter β, as described above, and appears to be consistent with the shift from LO to NLO. Notice that the LO (orange) band reflects the uncertainty in the NPLQCD prediction of the binding energy and does not include the theoretical uncertainty of the LETs. As required by the Levinson theorem for the case of a bound deuteron, the phase shifts generated by the LETs go through 180° at the origin. Comparing the NPLQCD results for phase shifts and the effective range function in the $^3S_1$ channel with those based on the LETs as visualized in Fig. 3, we end up with the following conclusions:

(1) First, as shown in the right panel of Fig. 3, only *positive* values of the scattering length appear to be consistent with the NPLQCD result for the deuteron binding energy quoted in Eq. (3.1) as opposed to the negative central value for $a^{(^3S_1)}$ reported in Ref. [9]. Our results for the inverse scattering length extracted from B_d by means of the LETs disagree with the NPLQCD ones given in Eq. (3.3), as can be inferred from the right panel of Fig. 3.

(2) While the lattice phase shifts at higher momenta are in reasonable agreement with the ones predicted by the LETs, their low-momentum behavior is incompatible (within the quoted errors) with that predicted by the LETs, as demonstrated in both panels in Fig. 3. In particular, the phase shift calculated on the lattice at the lowest considered momentum of $k \simeq 122$ MeV, $\delta = 38(^{+13}_{-11})(^{+23}_{-16})$ degrees, is a factor of 3 smaller than the corresponding value of $\delta = 111(\pm 5)$ degrees extracted from the LETs.

(3) An extrapolation of the lattice data to zero momenta in the left panel of Fig. 3 seems to indicate that the phase shift goes to zero. This would, however, contradict the existence of a bound state in this partial wave as a consequence of the Levinson theorem (or require shifting δ_{3S1} by 180 degrees in the entire plotted energy range, which would be inconsistent with the LETs).

One may raise a question whether the observed inconsistencies between the lattice-QCD results for phase shifts, and the LETs predictions could originate from underestimating the quark mass dependence of the NLO contact interaction by constraining the function $\beta(M_\pi)$ as described in the previous section. To clarify this issue, we have increased the allowed variation of β by a factor of 2, i.e., we set $\delta\beta = 1$ instead of $\delta\beta = 0.5$. This corresponds to the allowed variation of the strength of the short-range term at $M_\pi = 500$ MeV by $\pm 100\%$ as compared to its value at the physical point. The resulting predictions for the phase shifts and the effective range function are shown by the hatched blue light-shaded bands in Fig. 3. With the resulting uncertainty nearly covering the shift from our LO to NLO results, we expect such an error estimation to be too conservative. Still, none of our conclusions appear to be affected by employing this very conservative uncertainty estimation.

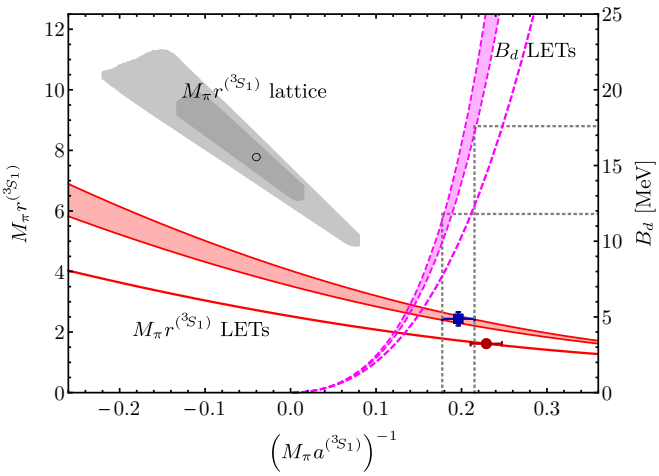

FIG. 4. Correlations between the inverse scattering length a^{-1}, effective range r and the binding energy in the ${}^3S_1$ partial wave induced by the one-pion exchange potential. The red solid and dashed magenta lines show the predictions of the LO LETs for $M_\pi r^{(^3S_1)}$ and B_d. The light-shaded bands between the red solid and dashed magenta lines visualize the predictions of the NLO LETs for $M_\pi r^{(^3S_1)}$ and B_d, respectively, and reflect the theoretical uncertainty estimated via the variation of β with $\delta\beta = 0.5$ as described in the text. The horizontal dotted lines specify the range of values for B_d consistent with the lattice-QCD results of Ref. [9] for this observable. The solid dark-red circle (blue rectangle) shows the LO (NLO) LET predictions for the effective range. The open black circle gives the result for the inverse scattering length and effective range reported by the NPLQCD Collaboration [9] while the grey area around it shows the estimated uncertainty from that paper. All results correspond to the Blatt-Biedenharn parametrization of the S-matrix [43].

We are now in the position to employ the LETs in order to extract the scattering length and the effective range from the deuteron binding energy calculated by the NPLQCD Collaboration. Such an extraction is possible because the effective range function does not possess poles at low momenta and, therefore, can be Taylor expanded around the origin.[4] In Fig. 4, we plot the deuteron binding energy and the effective range as functions of the inverse scattering length in units of the pion mass predicted by the LETs at LO (shown by the lines) and NLO (shown by the bands).

Specifically, the red band between two solid lines represents the NLO LET calculation for the effective range as a function of the inverse scattering length. Similarly, the magenta band between two dashed lines shows the deuteron binding energy versus the inverse scattering length at NLO. Further, the two horizontal dotted lines separate the region of the binding energies consistent with the NPLQCD result of Ref. [9], Eq. (3.1), for the binding energy. Projecting this area onto the x axis, as shown by the vertical lines, one obtains the corresponding values of the scattering length and the effective range from the LETs. In particular, we find

$$\begin{aligned}
\left(M_\pi a^{(^3S_1)}_{\text{LET, LO}}\right)^{-1} &= 0.229\left(^{+0.019}_{-0.018}\right), \\
\left(M_\pi a^{(^3S_1)}_{\text{LET, NLO}}\right)^{-1} &= 0.196\left(^{+0.014}_{-0.013}\right)\left(^{+0.007}_{-0.004}\right), \\
M_\pi r^{(^3S_1)}_{\text{LET, LO}} &= 1.62\left(^{+0.06}_{-0.06}\right), \\
M_\pi r^{(^3S_1)}_{\text{LET, NLO}} &= 2.44\left(^{+0.08}_{-0.08}\right)\left(^{+0.12}_{-0.17}\right),
\end{aligned} \tag{3.4}$$

which correspond to the following values in units of fm:

$$\begin{aligned}
a^{(^3S_1)}_{\text{LET, LO}} &= 1.915\left(^{+0.159}_{-0.147}\right)\ \text{fm}, \\
a^{(^3S_1)}_{\text{LET, NLO}} &= 2.234\left(^{+0.156}_{-0.144}\right)\left(^{+0.052}_{-0.072}\right)\ \text{fm}, \\
r^{(^3S_1)}_{\text{LET, LO}} &= 0.71\left(^{+0.02}_{-0.03}\right)\ \text{fm}, \\
r^{(^3S_1)}_{\text{LET, NLO}} &= 1.07\left(^{+0.03}_{-0.03}\right)\left(^{+0.05}_{-0.08}\right)\ \text{fm}.
\end{aligned} \tag{3.5}$$

Here, the errors in the first parentheses reflect the uncertainty in the value of the deuteron binding energy in Eq. (3.1) used as input. For the NLO results, we also give in the second parentheses an estimation of the theoretical uncertainty corresponding to the choice of $\delta\beta = 0.5$. Clearly, the above values are at variance with those extracted by the NPLQCD Collaboration and given in Eq. (3.3). In particular, our value for the effective range is about a factor of 3 smaller than the one found in Ref. [9]. Interestingly, the NLO LET prediction for the effective range is in excellent agreement with the assumed linear in M_π behavior of the quantity $M_\pi r^{(^3S_1)}$ conjectured in Ref. [19]; cf. Fig. 1 and the right panel of Fig. 8. For the sake of completeness, we also give the NLO LET results based on a more conservative uncertainty estimation, resulting by employing a weaker constraint on the allowed M_π dependence of the subleading contact interaction corresponding to the choice of $\delta\beta = 1$:

$$\begin{aligned}
\left(M_\pi a^{(^3S_1)}_{\text{LET, NLO}}\right)^{-1} &= 0.196\left(^{+0.014}_{-0.013}\right)\left(^{+0.018}_{-0.008}\right), \\
M_\pi r^{(^3S_1)}_{\text{LET, NLO}} &= 2.44\left(^{+0.08}_{-0.08}\right)\left(^{+0.21}_{-0.47}\right),
\end{aligned} \tag{3.6}$$

or

$$\begin{aligned}
a^{(^3S_1)}_{\text{LET, NLO}} &= 2.234\left(^{+0.156}_{-0.144}\right)\left(^{+0.093}_{-0.191}\right)\ \text{fm}, \\
r^{(^3S_1)}_{\text{LET, NLO}} &= 1.07\left(^{+0.03}_{-0.03}\right)\left(^{+0.09}_{-0.21}\right)\ \text{fm}
\end{aligned} \tag{3.7}$$

in units of fm.

To understand the origin of the disagreement between our results for the scattering length and effective range with those of Ref. [9], it is instructive to take a closer look at the procedure for their determination employed by the NPLQCD Collaboration. To this aim, a fit of the lattice phase-shift data at the two lowest energies and the deuteron pole was performed using the effective-range approximation (3.2). Note that the considered phase shifts and the deuteron pole correspond to momenta below the branch point of the t-channel cut due to the OPEP. For nonsingular potentials of a finite range, the applicability region of the effective range expansion is given by the inverse range of the interaction which determines the

[4]The effective range function does have a pole at $k \simeq 500$ MeV where the phase shift crosses zero, but these momenta are already beyond the region of the validity of the effective range expansion.

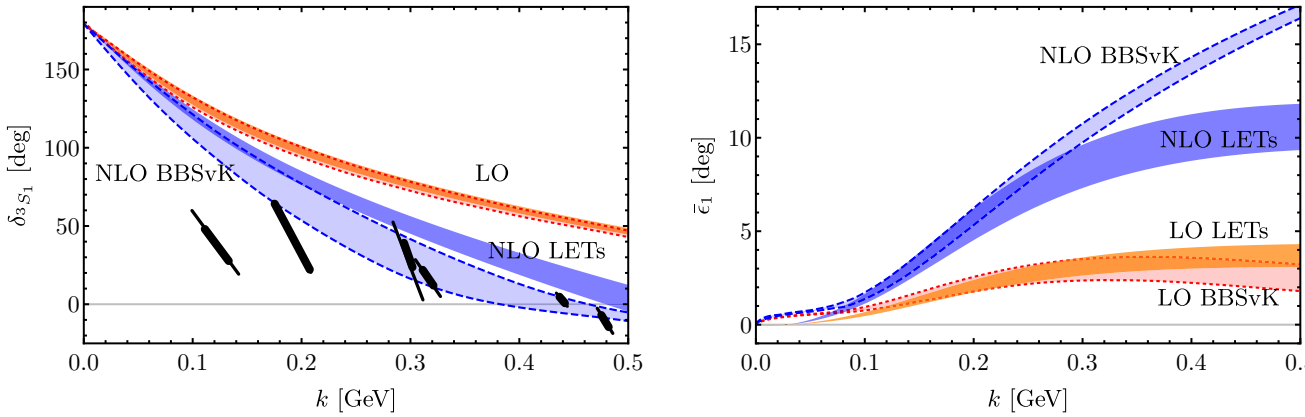

FIG. 5. Neutron-proton phase shifts in the $^3S_1$ channel (left panel) and the mixing angle $\bar{\epsilon}_1$ (right panel) at $M_\pi \sim 450$ MeV based on the LETs at LO and NLO in comparison with the results obtained in Ref. [9] using the EFT formulation of Ref. [10], labeled as BBSvK, at LO (light-shaded band between pink dotted lines) and NLO (light-shaded band between blue dashed lines). The results for the $^3S_1$ phase shift correspond to the Blatt-Biedenharn parametrization of the S-matrix [43] while the mixing parameter is shown for the Stapp parametrization to allow for the comparison with the results of Ref. [9]. For remaining notation see Fig. 3.

position of the first left-hand singularity. Consequently, the effective range and shape parameters may be expected to scale with the corresponding powers of the pion mass. For example, for the physical value of the pion mass, one has $r^{(^1S_0)} = 1.9 M_\pi^{-1}$ and $r^{(^3S_1)} = 1.2 M_\pi^{-1}$. The very large value of the effective range reported by the NPLQCD Collaboration, $r^{(^3S_1)} = 7.8 M_\pi^{-1}$, either indicates that the range of the nuclear force is considerably larger than that of the OPEP or signals the appearance of a pole in the effective-range function in the near-threshold region.[5] In both cases, the applicability range of the effective range expansion of $k \cot\delta$ would be significantly smaller than one may expect based on the position of the left-hand cut due to the OPEP. As a consequence, the solution for $a^{(^3S_1)}$ and $r^{(^3S_1)}$ reported in Ref. [9] and listed in Eq. (3.3) is not self-consistent in the sense that it is obtained by fitting the effective range approximation to the data points outside of its validity region, which can be roughly estimated as $|k| \lesssim 2/r^{(^3S_1)} \sim 0.26 M_\pi$. Specifically, the deuteron binding momentum at $M_\pi \simeq 450$ MeV is of the order of $\gamma \sim 0.3 M_\pi$, whereas the phase-shift data employed in the analysis correspond to $k \sim 0.27 M_\pi$ and $k \sim 0.42 M_\pi$.

To get further insights into this issue, consider the two roots of the quadratic equation $-1/a + rk^2/2 - ik = 0$ which determines the pole positions of the scattering amplitude within the effective-range approximation,

$$k_1 = \frac{i}{r}\left(1 + \sqrt{1 - \frac{2r}{a}}\right) \simeq i\left(\frac{2}{r} - \frac{1}{a}\right),$$
$$k_2 = \frac{i}{r}\left(1 - \sqrt{1 - \frac{2r}{a}}\right) \simeq \frac{i}{a}\left(1 + \frac{r}{2a}\right), \tag{3.8}$$

where we have expanded the square root in powers of r/a and neglected terms of order $\mathcal{O}((r/a)^2)$. This is justified both for the physical value of the pion mass and for the solution given in Eq. (3.3), since in both cases one has $|r/a| \sim 0.3$. At the physical pion mass, the second root yields the deuteron binding momentum $k_2 \simeq 45i$ MeV while the first root, $k_1 \simeq 200i$ MeV, lies outside of the applicability region of the effective range expansion and is an artifact of the effective range approximation. In particular, it disappears or changes the position upon including higher-order terms in the effective range expansion. On the contrary, for the solution in Eq. (3.3) at $M_\pi \simeq 450$ MeV, the deuteron pole corresponds to the first root, $k_1 \simeq 135i$ MeV, where the dominant contribution comes from the effective range. Meanwhile, because the scattering length in Eq. (3.3) is negative, the second root corresponds to the momentum $k_2 \simeq -15i$ MeV lying on the imaginary axis in the lower half-plane. Therefore, the results of Ref. [9] imply the existence of a shallow virtual state with excitation energy less than 0.5 MeV in addition to the deuteron, which is not supported by our analysis based on the LETs.

Finally, it is interesting to compare our results based on the LETs with the ones obtained using an alternative approach proposed in Ref. [10], which will be referred to as BBSvK, where the expansion of the nuclear force around the chiral limit was employed; see, however, Ref. [28] for a criticism. This approach was used in Ref. [9] to calculate the phase shifts and the mixing angle in the $^3S_1$–$^3D_1$ channel. A comparison of results from the two approaches is presented in Fig. 5.

While the $^3S_1$ phase shift and the mixing angle show a very similar behavior at LO, there are more sizable differences at NLO. Notice that apart from the different treatment of pions, the two approaches also differ in the way the NLO short-range interaction is taken into account. In particular, in Ref. [9], the strength of this subleading short-range term was adjusted to fit the lattice phase shifts. In contrast, in our approach, the strength of the subleading contact interaction β is determined by the value of the effective range at the physical point, while its allowed M_π dependence at unphysical pion masses is used to estimate the theoretical uncertainty as explained in Sec. II B. This procedure ensures that both the LO and NLO LET results depend on a single unknown parameter. We further emphasize

[5]For example, such a pole very close to threshold appears in the spin-doublet S-wave channel for neutron-deuteron scattering.

that the low-energy behavior of the mixing angle found in Ref. [9] and shown in the right panel of Fig. 5 seems to be at variance with the expected threshold behavior for this quantity, $\bar{\epsilon}_1 \sim k^3$ (for details see, e.g., [31]). Regardless of these differences, the two approaches yield similar numerical results for the $^3S_1$ phase shift and the mixing angle $\bar{\epsilon}_1$ in the considered range of momenta. The values of the scattering length and effective range extracted in Ref. [9] from the lattice data using the framework of Ref. [10] read

$$\begin{aligned} a^{(^3S_1)}_{\text{BBSvK, LO}} &= 1.94(09)(17)\ \text{fm}, \\ a^{(^3S_1)}_{\text{BBSvK, NLO}} &= 2.72(22)(27)\ \text{fm}, \\ r^{(^3S_1)}_{\text{BBSvK, LO}} &= 0.674(17)(29)\ \text{fm}, \\ r^{(^3S_1)}_{\text{BBSvK, NLO}} &= 1.43(12)(13)\ \text{fm}, \end{aligned} \tag{3.9}$$

where the uncertainties in the first and second parentheses correspond to the statistical and systematic uncertainties of the lattice results. As already pointed out, the LO values are in agreement with our LO predictions given in Eq. (3.5), while the deviations at NLO and, in particular, the large value of the effective range are presumably caused by an attempt to reproduce the lattice-QCD result for the $^3S_1$ phase shift at $k \simeq 0.2$ GeV within the BBSvK approach. We further emphasize that the authors of Ref. [9] do not elaborate on possible sources of inconsistency between the two sets of values reported in their work and listed in Eqs. (3.3) and (3.9).

B. The $^1S_0$ channel

We now turn to the spin-singlet channel. In Fig. 6, we confront the phase shifts extracted based on the LETs with the lattice-QCD results for the $^1S_0$ partial wave. Here we apply the same procedure as in the $^3S_1$ channel and use the NPLQCD result for the dineutron binding energy [9],

$$B_{nn} = 12.5\left(^{+3.0}_{-5.0}\right)\ \text{MeV}, \tag{3.10}$$

as input to fix the short-range interaction at LO. The NLO short-range interaction is again taken into account by means of resonance saturation, see Eq. (2.13), with the strength β being determined by the effective range at the physical point. The allowed M_π dependence of β is specified by Eq. (2.14), and the blue dark-shaded bands in Fig. 6 correspond to the choice $\delta\beta = 0.5$. Notice that the shift in the predictions when going from LO to NLO is now much larger than in the spin-triplet channel, which is in line with the lower predictive power of the LETs in the $^1S_0$ partial wave. Consequently, we believe that a variation of the strength β with $\delta\beta = 0.5$ does not provide a realistic estimation of the theoretical uncertainty at NLO in this channel. To have a more conservative estimation, we will allow for a larger M_π dependence in this channel and set $\delta\beta = 1$ as visualized by the hatched blue light-shaded bands in Fig. 6.

As shown in Fig. 6, we arrive at similar conclusions as in the case of the spin-triplet channel. While our NLO LET predictions for $k > 300$ MeV are in very good agreement with the phase shifts calculated by the NPLQCD Collaboration, there is a clear discrepancy for the two lowest values of the momentum k. In particular, for the lowest momentum of $k \sim 100$ MeV, the phase shift from the NLO LETs is roughly a factor of 2 larger than that from the lattice-QCD analysis. Similarly to the $^3S_1$ channel, the predictions of the LETs based on the dineutron binding energy are only compatible with positive values of the scattering length; see the right panel of Fig. 6. Specifically, we obtain

$$\begin{aligned} \left(M_\pi a^{(^1S_0)}_{\text{LET, LO}}\right)^{-1} &= 0.244\left(^{+0.026}_{-0.051}\right), \\ \left(M_\pi a^{(^1S_0)}_{\text{LET, NLO}}\right)^{-1} &= 0.175\left(^{+0.013}_{-0.028}\right)\left(^{+0.024}_{-0.008}\right), \\ M_\pi r^{(^1S_0)}_{\text{LET, LO}} &= 0.90\left(^{+0.14}_{-0.06}\right), \\ M_\pi r^{(^1S_0)}_{\text{LET, NLO}} &= 2.86\left(^{+0.27}_{-0.12}\right)\left(^{+0.27}_{-0.74}\right), \end{aligned} \tag{3.11}$$

which correspond to the following values in units of fm:

$$\begin{aligned} a^{(^1S_0)}_{\text{LET, LO}} &= 1.797\left(^{+0.479}_{-0.171}\right)\ \text{fm}, \\ a^{(^1S_0)}_{\text{LET, NLO}} &= 2.501\left(^{+0.481}_{-0.174}\right)\left(^{+0.123}_{-0.304}\right)\ \text{fm}, \\ r^{(^1S_0)}_{\text{LET, LO}} &= 0.40\left(^{+0.06}_{-0.03}\right)\ \text{fm}, \\ r^{(^1S_0)}_{\text{LET, NLO}} &= 1.25\left(^{+0.12}_{-0.05}\right)\left(^{+0.12}_{-0.32}\right)\ \text{fm}. \end{aligned} \tag{3.12}$$

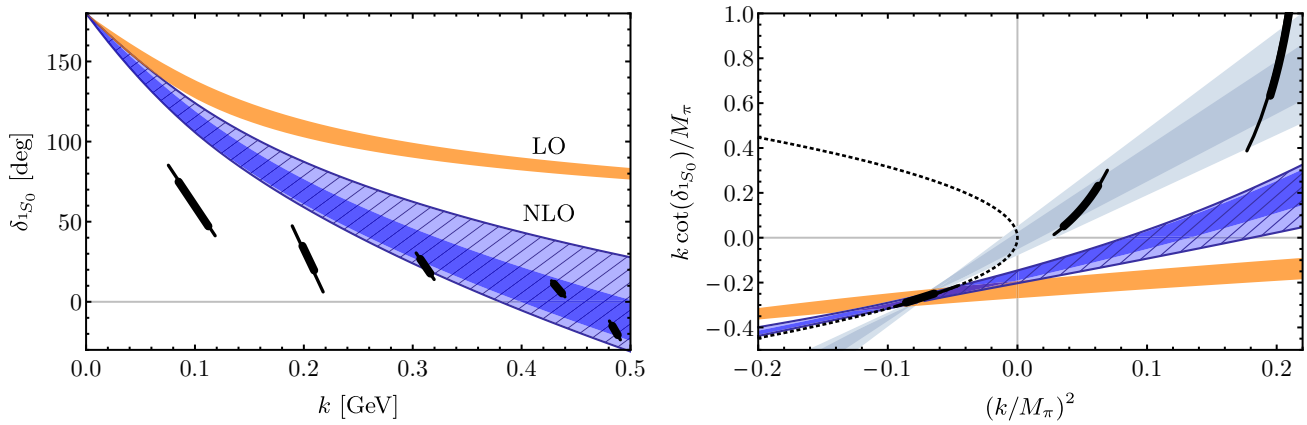

FIG. 6. Two-nucleon phase shifts (left panel) and the effective-range function (right panel) in the $^1S_0$ channel calculated on the lattice at $M_\pi \sim 450$ MeV [9] in comparison with the predictions based on the LETs at LO and NLO using the NPLQCD result for the dineutron binding energy B_{nn} as input. For notation see Fig. 3.

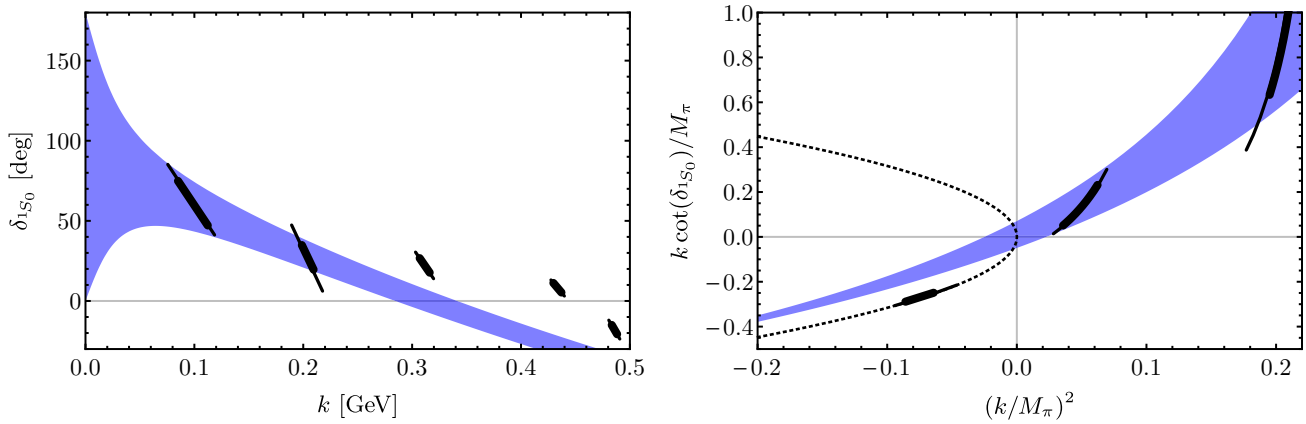

FIG. 7. Two-nucleon phase shifts (left panel) and the effective-range function (right panel) in the $^1S_0$ channel calculated on the lattice at $M_\pi \sim 450$ MeV [9] in comparison with the predictions based on the LETs at NLO (blue shaded bands) using the scattering length in Eq. (3.14) as input. For remaining notation see Fig. 3.

Here, the errors at LO and in the first parentheses at NLO correspond to the uncertainty in the dineutron binding energy while the ones in the second parentheses at NLO reflect the unknown M_π dependence of β subject to the constraint $\delta\beta = 1$. These results are in conflict with the NPLQCD determination based on the effective range expansion, namely [9]

$$\begin{aligned}\left(M_\pi a^{(^1S_0)}\right)^{-1} &= 0.021\left(^{+0.028}_{-0.036}\right)\left(^{+0.032}_{-0.063}\right),\\ M_\pi r^{(^1S_0)} &= 6.7\left(^{+1.0}_{-0.8}\right)\left(^{+2.0}_{-1.3}\right).\end{aligned} \tag{3.13}$$

Again, we believe that the analysis performed by the NPLQCD Collaboration and based on the effective range approximation is not self-consistent. All arguments given in the previous section apply to the $^1S_0$ channel too, even though our conclusions in this case are somewhat less stringent due to the lower accuracy of the LETs. To further elaborate on this point and to provide an assessment of the robustness of our conclusions, we have redone the calculations by using the lattice phase shifts instead of the dineutron binding energy as input. Specifically, we vary the scattering length, which is now used as input for the LETs at NLO, in the range consistent with the lattice-QCD phase shifts at the two lowest energies. The resulting phase shifts, corresponding to the inverse scattering length in the range of

$$\left(M_\pi a^{(^1S_0)}\right)^{-1} = -0.01 \pm 0.06, \tag{3.14}$$

are shown in the left panel of Fig. 7. Here, we set $\delta\beta = 0$, and the width of the band reflects the uncertainty of the lattice-QCD phase shifts used as input. Notice that while the NPLQCD value of the inverse scattering length given in Eq. (3.13) is indeed consistent with the range of values in Eq. (3.14), the obtained solutions correspond to the bound (virtual) state binding energy of $B_{nn} < 0.5$ MeV ($B_{nn}^{\text{virtual}} < 0.6$ MeV), which is in conflict with the lattice-QCD prediction. The apparent bound state corresponding to the leftmost intersection point of the gray bands with the unitarity term $ik/M_\pi = -\sqrt{-(k/M_\pi)^2}$ in the right panel of Fig. 6 is an artifact of the effective range approximation.

Finally, it is interesting to compare our results for the scattering length and effective range with the values obtained in Ref. [9] within the Kaplan-Savage-Wise (KSW) approach to chiral EFT [44,45], namely

$$\begin{aligned}a^{(^1S_0)}_{\text{KSW, NLO}} &= 2.62(07)(16)\ \text{fm},\\ a^{(^1S_0)}_{\text{KSW, NNLO}} &= 2.99(07)(15)\ \text{fm},\\ r^{(^1S_0)}_{\text{KSW, NLO}} &= 1.320(18)(38)\ \text{fm},\\ r^{(^1S_0)}_{\text{KSW, NNLO}} &= 1.611(42)(83)\ \text{fm}.\end{aligned} \tag{3.15}$$

Notice that the effective range vanishes at LO in the KSW approach, and the number of independent parameters fitted to lattice data is equal to 1, 2, and 3 at LO, NLO, and next-to-next-to-leading order (NNLO), respectively. Our NLO LET results are in excellent agreement with the NLO KSW values and also nearly consistent with the NNLO KSW results.

IV. THE EFFECTIVE RANGE AT UNPHYSICAL PION MASSES

As already discussed, Ref. [19] conjectured that the effective range calculated on lattice at $M_\pi \simeq 800$ MeV and expressed in units of the pion mass may be extrapolated to the physical point by a linear function of M_π. We are now in the position to test this hypothesis by an explicit calculation based on the LETs. Using the NN bound state energies calculated on the lattice at $M_\pi \simeq 300$ MeV [8], $M_\pi \simeq 390$ MeV [7], $M_\pi \simeq 450$ MeV [9], and $M_\pi \simeq 510$ MeV [21], we employ the LETs at NLO to predict the values of the effective range in the $^1S_0$ and $^3S_1$ partial waves. The results are visualized in Fig. 8.[6] Note that the last point in

[6]The value for $M_\pi r^{(^1S_0)}$ at $M_\pi \simeq 800$ MeV given in Ref. [19], $M_\pi r^{(^1S_0)} = 4.61\left(^{+0.29}_{-0.31}\right)\left(^{+0.24}_{-0.26}\right)$, is somewhat different from the one plotted in their Fig. 11 and corresponding to the linear extrapolation specified in Eq. (8) of that work. The lattice-QCD result at $M_\pi \simeq 800$ MeV shown in the left panel of Fig. 8 is based on the linear extrapolation specified in Eq. (8) of Ref. [19].

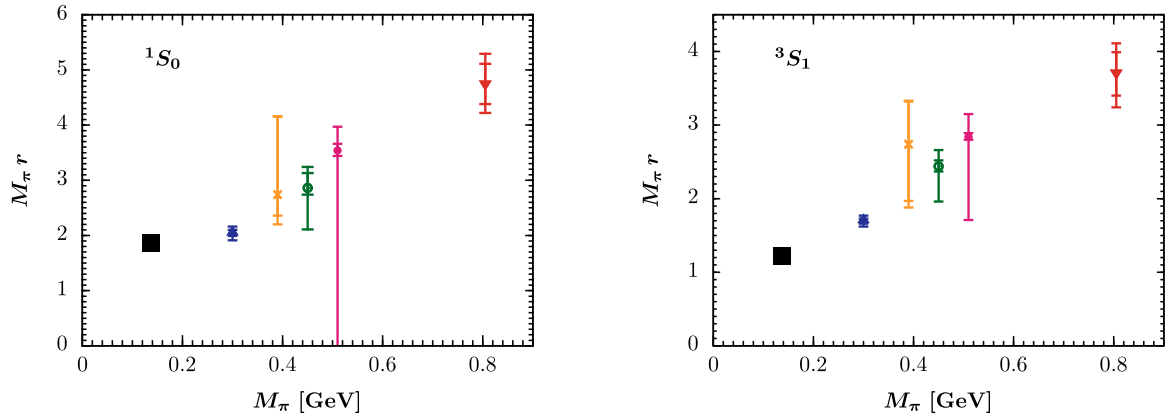

FIG. 8. Nucleon-nucleon effective range ($M_\pi r$) in the ^{1}S$_0$ (left panel) and ^{3}S$_1$ (right panel) partial waves predicted based on the next-to-leading order LETs using the bound state energies calculated on the lattice as input. Blue open triangles, orange crosses, green open circles and purple solid circles show $M_\pi r$ for the binding energies at $M_\pi \simeq 300$ MeV [8], $M_\pi \simeq 390$ MeV [7], $M_\pi \simeq 450$ MeV [9], and $M_\pi \simeq 510$ MeV [21], respectively. The uncertainty of our results for $M_\pi r$ is twofold: the smaller error bars reflect the uncertainty of the lattice results for the binding energies used as input while larger ones correspond to the theoretical uncertainty of the LETs estimated by setting $\delta\beta = 1$ and the uncertainty of the lattice results added in quadrature. Red solid triangles correspond to the NPLQCD results for $M_\pi r$ at $M_\pi \simeq 800$ MeV [18]. The black squares show the empirical values of the effective range at the physical pion mass [31,46].

both panels at $M_\pi \simeq 800$ MeV represents the result of lattice calculations by the NPLQCD Collaboration [19], while the LETs are already beyond their range of validity at such heavy pion masses. As seen from the right panel of Fig. 8, the NLO LETs predictions for the effective range in the ^{3}S$_1$ partial wave are in very good agreement with the linear in M_π behavior of the quantity $M_\pi r^{(^3S_1)}$. Interestingly, the lattice data point at $M_\pi \simeq 800$ MeV is consistent with the NLO LET results linearly extrapolated to higher pion masses. The results from the LETs for the ^{1}S$_0$ partial wave, although less conclusive due to larger uncertainties, are also generally consistent with the linear in M_π behavior of $M_\pi r^{(^1S_0)}$. We note at this point that the lattice data at $M_\pi \simeq 800$ MeV were obtained in Ref. [18] by using the effective range approximation. The same procedure was employed by the NPLQCD Collaboration to extract the scattering length and effective range at $M_\pi \simeq 450$ MeV and is criticized in this work. It is conceivable that the data at $M_\pi \simeq 800$ MeV might also suffer from underestimated systematic uncertainties.

V. SUMMARY

In this paper, we have employed the low-energy theorems for NN scattering, which have been generalized in Ref. [24] to the case of unphysical pion masses, to analyze the recent lattice-QCD results at $M_\pi \simeq 450$ MeV reported by the NPLQCD Collaboration [9]. The pertinent results of our work can be summarized as follows.

(1) We have used the LETs along with the lattice-QCD results for the deuteron and dineutron binding energies in order to extract the energy behavior of the NN phase shifts in the $^3S_1$ and $^1S_0$ partial waves and the mixing angle $\bar{\epsilon}_1$ at $M_\pi \simeq 450$ MeV. Our LO and NLO calculations suggest a good (fair) convergence of our theoretical approach in the spin-triplet (spin-singlet) channel. In both channels, the resulting phase shifts are in good agreement with the lattice-QCD results of Ref. [9] for momenta of $k > 300$ MeV, but are inconsistent with the lattice-QCD predictions at lower energies.

(2) We have used the LETs to extract the values of the scattering length and effective range in the $^3S_1$ and $^1S_0$ partial waves from the bound state energies obtained on the lattice. The extracted value of $M_\pi r^{(^3S_1)}$ is in excellent agreement with the linear in M_π behavior of this quantity conjectured in Ref. [19]. On the other hand, our results are in strong disagreement with the values obtained by the NPLQCD Collaboration from fits to the lattice-QCD data based on the effective range approximation. We have argued that the very large values for the effective range found in Ref. [9] make the effective range approximation invalid in the energy region corresponding to the lattice data.

(3) Our results for phase shifts, scattering lengths, and effective ranges agree reasonably well with those obtained in Ref. [9] by analyzing lattice-QCD data within the various EFT approaches.

Given considerable evidence of a bound dineutron and a stronger bound deuteron at heavy pion masses [7–9,21], our findings indicate that the lattice-QCD calculations of the NN phase shifts of Ref. [9] using the extended Lüscher approach may possibly suffer from underestimated systematic errors at the lowest considered energies. While this seems less likely to us, the origin of the observed inconsistencies may also be related to the incorrect determination of the deuteron and dineutron binding energies on the lattice; see Refs. [22,47] for related discussions.

In addition, using lattice results for the binding energies of the deuteron and dineutron at various pion masses as input [7–9,21], we demonstrate that the effective range expressed in units of the pion mass behaves as a linear function of M_π.

Our work demonstrates that the LETs provide a useful tool to analyze lattice QCD results for the NN system by allowing one to extract the scattering phase shifts from the calculated bound state energies and/or test consistency of lattice calculations if several observables are computed for a given value of the pion mass.

ACKNOWLEDGMENTS

We would like to thank Jambul Gegelia for sharing his insights into the topic discussed here and for a careful reading of the manuscript. We are also grateful to the organizers of the YIPQS Long-term and Nishinomiya-Yukawa Memorial International Workshop on "Computational Advances in Nuclear and Hadron Physics" at Yukawa Institute for Theoretical Physics, Kyoto University and to the organizers of the INT-16-1 program "Nuclear physics from lattice QCD" at INT Seattle, where a part of this work was carried out. Work supported in part by the ERC (project 259218 NuclearEFT), the BMBF (Verbundprojekt 05P2015 - NUSTAR R&D). The work of V.B. was supported by the DFG (grant BA 5443/1-1).

[1] U.-G. Meißner, Sci. Bull. **60**, 43 (2015).
[2] H. Oberhummer, A. Csoto, and H. Schlattl, Nucl. Phys. A **689**, 269 (2001).
[3] E. Epelbaum, H. Krebs, T. A. Lähde, D. Lee, and U.-G. Meißner, Phys. Rev. Lett. **110**, 112502 (2013).
[4] E. Epelbaum, H. Krebs, T. A. Lähde, D. Lee, and U.-G. Meißner, Eur. Phys. J. A **49**, 82 (2013).
[5] P. F. Bedaque, T. Luu, and L. Platter, Phys. Rev. C **83**, 045803 (2011).
[6] J. C. Berengut, E. Epelbaum, V. V. Flambaum, C. Hanhart, U.-G. Meißner, J. Nebreda, and J. R. Peláez, Phys. Rev. D **87**, 085018 (2013).
[7] S. R. Beane, E. Chang, W. Detmold, H. W. Lin, T. C. Luu, K. Orginos, A. Parreño, M. J. Savage, A. Torok, and A. Walker-Loud (NPLQCD Collaboration), Phys. Rev. D **85**, 054511 (2012).
[8] T. Yamazaki, K.-i. Ishikawa, Y. Kuramashi, and A. Ukawa, Phys. Rev. D **92**, 014501 (2015).
[9] K. Orginos, A. Parreño, M. J. Savage, S. R. Beane, E. Chang, and W. Detmold, Phys. Rev. D **92**, 114512 (2015).
[10] S. R. Beane, P. F. Bedaque, M. J. Savage, and U. van Kolck, Nucl. Phys. A **700**, 377 (2002).
[11] S. R. Beane and M. J. Savage, Nucl. Phys. A **713**, 148 (2003).
[12] E. Epelbaum, U.-G. Meißner, and W. Glöckle, Nucl. Phys. A **714**, 535 (2003).
[13] S. R. Beane and M. J. Savage, Nucl. Phys. A **717**, 91 (2003).
[14] E. Epelbaum, U.-G. Meißner, and W. Glöckle, arXiv:nucl-th/0208040.
[15] J. W. Chen, T. K. Lee, C.-P. Liu, and Y. S. Liu, Phys. Rev. C **86**, 054001 (2012).
[16] J. Soto and J. Tarrus, Phys. Rev. C **85**, 044001 (2012).
[17] E. Epelbaum and J. Gegelia, PoS CD **12**, 090 (2013).
[18] S. R. Beane, E. Chang, S. D. Cohen, W. Detmold, H. W. Lin, T. C. Luu, K. Orginos, A. Parreño, M. J. Savage, and A. Walker-Loud (NPLQCD Collaboration), Phys. Rev. D **87**, 034506 (2013).
[19] S. R. Beane, E. Chang, S. D. Cohen, W. Detmold, P. Junnarkar, H. W. Lin, T. C. Luu, K. Orginos, A. Parreño, M. J. Savage, and A. Walker-Loud (NPLQCD Collaboration), Phys. Rev. C **88**, 024003 (2013).
[20] E. Berkowitz *et al.*, arXiv:1508.00886.
[21] T. Yamazaki, K.-i. Ishikawa, Y. Kuramashi, and A. Ukawa, Phys. Rev. D **86**, 074514 (2012).
[22] T. Inoue *et al.* (HAL QCD Collaboration), Nucl. Phys. A **881**, 28 (2012).
[23] V. V. Flambaum and R. B. Wiringa, Phys. Rev. C **76**, 054002 (2007).
[24] V. Baru, E. Epelbaum, A. A. Filin, and J. Gegelia, Phys. Rev. C **92**, 014001 (2015).
[25] T. D. Cohen and J. M. Hansen, Phys. Rev. C **59**, 13 (1999).
[26] T. D. Cohen and J. M. Hansen, Phys. Rev. C **59**, 3047 (1999).
[27] J. V. Steele and R. J. Furnstahl, Nucl. Phys. A **645**, 439 (1999).
[28] E. Epelbaum and J. Gegelia, Eur. Phys. J. A **41**, 341 (2009).
[29] E. Epelbaum and J. Gegelia, PoS CD **09**, 077 (2009).
[30] E. Epelbaum, arXiv:1001.3229.
[31] J. J. de Swart, C. P. F. Terheggen, and V. G. J. Stoks, arXiv:nucl-th/9509032.
[32] H. van Haeringen and L. P. Kok, Phys. Rev. A **26**, 1218 (1982).
[33] E. Epelbaum and J. Gegelia, Phys. Lett. B **716**, 338 (2012).
[34] E. Epelbaum, A. M. Gasparyan, J. Gegelia, and H. Krebs, Eur. Phys. J. A **51**, 71 (2015).
[35] V. G. Kadyshevsky, Nucl. Phys. B **6**, 125 (1968).
[36] V. Baru, E. Epelbaum, A. A. Filin, J. Gegelia, and A. V. Nefediev, Phys. Rev. D **92**, 114016 (2015).
[37] J. M. Blatt and J. D. Jackson, Phys. Rev. **76**, 18 (1949).
[38] H. A. Bethe, Phys. Rev. **76**, 38 (1949).
[39] B. Midya , J. Evrard, S. Abramowicz, O. L. R. Suárez, and J.-M. Sparenberg, Phys. Rev. C **91**, 054004 (2015).
[40] M. Lüscher, Commun. Math. Phys. **105**, 153 (1986).
[41] M. Lüscher, Nucl. Phys. B **354**, 531 (1991).
[42] R. A. Briceño, Z. Davoudi, T. C. Luu, and M. J. Savage, Phys. Rev. D **88**, 114507 (2013).
[43] J. M. Blatt and L. C. Biedenharn, Rev. Mod. Phys. **24**, 258 (1952).
[44] D. B. Kaplan, M. J. Savage, and M. B. Wise, Nucl. Phys. B **534**, 329 (1998).
[45] D. B. Kaplan, M. J. Savage, and M. B. Wise, Phys. Lett. B **424**, 390 (1998).
[46] M. P. Valderrama and E. R. Arriola, Phys. Rev. C **72**, 044007 (2005).
[47] T. Iritani (HAL QCD Collaboration), arXiv:1511.05246.